



Magnetic Resonance Spectroscopy Findings of Intracranial Chondroma and Chondrosarcoma with a Non-skull Base Origin: A Report of Two Cases

Behzad Amanpour-Gharaei¹, Shirin Haghshenas Bilehsavar², Ahmad Pour-Rashidi³, Mohsen Izanlou⁴, Yasaman Bastanipour⁵, Hassan Hashemi⁶, Mohammad Ali Oghabian⁷, Elham Nazar⁸ and Samira Raminfard^{9,*}

¹Cancer Biology Research Center, Cancer Institute, Tehran University of Medical Sciences, Tehran, Iran

²Center of Functionally Integrative Neuroscience, Aarhus University, Aarhus, Denmark

³Department of Neurosurgery, Sina Hospital, Tehran University of Medical Sciences, Tehran, Iran

⁴Department of Radiology, North Khorasan University of Medical Sciences, North Khorasan, Iran

⁵Department of Medical Physics and Radiology, North Khorasan University of Medical Sciences, Bojnurd, Iran

⁶Department of Radiology, School of Medicine, Advanced Diagnostic and Interventional Radiology Research Center, Imam Khomeini Hospital, Tehran University of Medical Sciences, Tehran, Iran

⁷Neuroimaging and Analysis Group, Research Center for Molecular and Cellular Imaging, Advanced Medical Technologies and Equipment Institute, Tehran University of Medical Sciences, Tehran, Iran

⁸Department of Pathology, Sina Hospital, Tehran University of Medical Sciences, Tehran, Iran

⁹Advanced Diagnostic and Interventional Radiology Research Center, Imam Khomeini Hospital Complex, Tehran University of Medical Sciences, Tehran, Iran

*Corresponding author: Advanced Diagnostic and Interventional Radiology Research Center, Imam Khomeini Hospital Complex, Tehran University of Medical Sciences, Tehran, Iran. Email: samira.raminfard@gmail.com

Received 2022 November 19; Revised 2023 July 29; Accepted 2023 August 02.

Abstract

Introduction: Intracranial chondroma and chondrosarcoma are very rare tumors that mainly originate from the base of the skull. Advanced neuroimaging studies, including magnetic resonance spectroscopy (MRS), play a pivotal role in both tumor diagnosis and presurgical planning.

Case Presentation: We present two cases of intracranial cartilaginous tumors, including a chondroma and a chondrosarcoma, both of which presented with severe headaches. Due to inconclusive conventional MRI and MRS results, they were both primarily diagnosed as intra-axial brain tumors. However, pathological reports later confirmed the diagnosis of a chondroma and a chondrosarcoma.

Conclusion: Based on the present findings, the use of advanced neuroimaging techniques, such as MRS, may improve diagnostic accuracy. We believe that MRS can play a significant role in the surgical planning of similar cases. Also, reporting rare cases worldwide can contribute to the improvement of radiographic diagnosis.

Keywords: Chondroma, Chondrosarcoma, MRI, MRS

1. Introduction

Chondroma is a well-known benign tumor that commonly occurs in the extremities. However, it may be also found in less common locations, such as the brain and cranial vault. According to previous studies, the incidence rate of chondroma is almost 0.2 - 0.5% of all intracerebral tumors (1). Most cases of intracranial chondromas have been reported in the skull base, the convexity of the dura mater, or the falx cerebri. These tumors are believed to originate from the cartilage of the synchondroses.

Intracranial chondromas are rare, and those originating from the cranial vault are even less common (2).

Chondrosarcomas are rare malignant tumors that are most commonly diagnosed in the pelvic bones and the epiphyses of long bones. Only 7% of all chondrosarcomas originate from the craniocervical region. Chondrosarcomas are slow-growing tumors, and intracranial chondrosarcomas originate from primitive mesenchymal cells in the craniocervical junction or the skull base (3). The role of computed tomography (CT) scans

and magnetic resonance imaging (MRI) in the diagnosis of intracranial chondromas and chondrosarcomas cannot be neglected. Functional MRI (fMRI) (4) and magnetic resonance spectroscopy (MRS) (5) can be also used for the diagnosis of these tumors, as well as presurgical planning.

In this study, we present two cases of intracranial cartilaginous tumors, including one case of chondroma and one case of chondrosarcoma, presenting with severe headaches and compare their clinical characteristics and imaging findings.

2. Clinical Presentation

2.1. Case 1

A 26-year-old female was admitted to our medical center with chronic headache as her chief medical complaint. The patient reported experiencing a persistent headache located in the right frontal area of the calvaria, which was unresponsive to routine analgesics. She had been experiencing the headache for nearly six months, and it had worsened over the last three months. She had no history of medical diseases and also reported no history of trauma or radiation exposure.

The patient's previous conventional brain MRI revealed the presence of a brain mass, which was suspected to be an intracranial tumor. However, it was not specified whether the tumor was intra- or extra-axial. Upon admission, she underwent physical and neurological examinations, which were found to be normal. Tumor mapping using fMRI, diffusion tensor imaging (DTI), MRS, and conventional MRI was ordered for presurgical planning. The MRI scan was performed using the 3.0T MR system (Discovery MR750, GE Healthcare). In the structural images, an intracranial lesion was observed in the right frontal lobe and pre-central region. Although the lesion did not exhibit evident enhancement in post-contrast T1 images, it displayed hyperintense regions in T2 images. There was no specific edematous area in the peripheral region. The absence of brain parenchyma between the lesion and the meningeal membrane in the coronal and sagittal planes confirmed that the lesion was extra-axial (Figure 1A).

Single-voxel spectroscopy (SVS) was performed on the lesion and the contralateral hemisphere for comparison, using a voxel size of $20 \times 20 \times 20$ mm³, a repetition time (TR) of 1500 ms, echo times (TE) of 144 and 35 ms, and a number of excitations (NEX) of 128. Outer volume

suppression was performed using six saturation bands placed around the voxel. To achieve field homogeneity, automatic shimming was applied, resulting in water peak line widths within the voxel that were typically less than 8 Hz. Water resonance suppression was achieved using a chemical shift selective suppression (CHESS) pulses. The results of moderate-TE MRS showed three distinct peaks at 2.02, 3, and 3.2 ppm, respectively, as well as an inverted doublet peak at 1.3 ppm, corresponding to lactate.

Compared to the normal voxel, the concentration of the metabolite at 2 ppm, which is typically associated with N-acetylaspartate (NAA), was found to be lower in the lesion. The level of choline (Cho) at 3.2 ppm, with an area under the peak of 14, decreased compared to the Cho level in the contralateral normal voxel, with an area under the peak of 24. The creatinine (Cr) peak also significantly decreased. The short TE spectra showed four discrete peaks, a positive doublet peak at 1.3 ppm, and three single peaks at 2, 3, and 3.2 ppm, which were related to lactate, NAA, Cr, and Cho, respectively (Figure 1B).

The multi-voxel 2D MRS sequence (TR = 1500 ms, TE = 144 ms, NEX = 2) produced a 16×16 transversely oriented matrix, defined by phase encoding with a field of view (FOV) of 20×20 cm and a voxel size of $12.5 \times 12.5 \times 15$ mm. The imaging plane was positioned to include the abnormality within the volume of interest (VOI), resulting in maps with 5×7 spectra. Six outer volume saturation bands were arranged around the VOI to optimize the suppression of lipids and brain tissue. Automated 3D localized shimming was also used to optimize the magnetic homogeneity and improve the accuracy and consistency of spectral measurements over the VOI. The spectra showed the same peaks as the single voxel in different portions of the lesion (Figure 1C).

In the MRS map, the peripheral area of the lesion had no abnormal metabolic features. In other words, the peripheral area was not infiltrated by tumor cells. This commonly occurs in extra-axial tumors, such as meningioma or metastasis. However, as previously described, no strong enhancement was observed, which excluded the possibility of a meningeal tumor or metastasis. Finally, based on the structural MRI and MRS findings, the radiological differential diagnosis included extra-axial lesions, such as hemangiopericytoma, which is the second most common type of meningeal tumor after meningioma. The macroscopic impression of the tumor during surgery suggested a cartilaginous origin. The

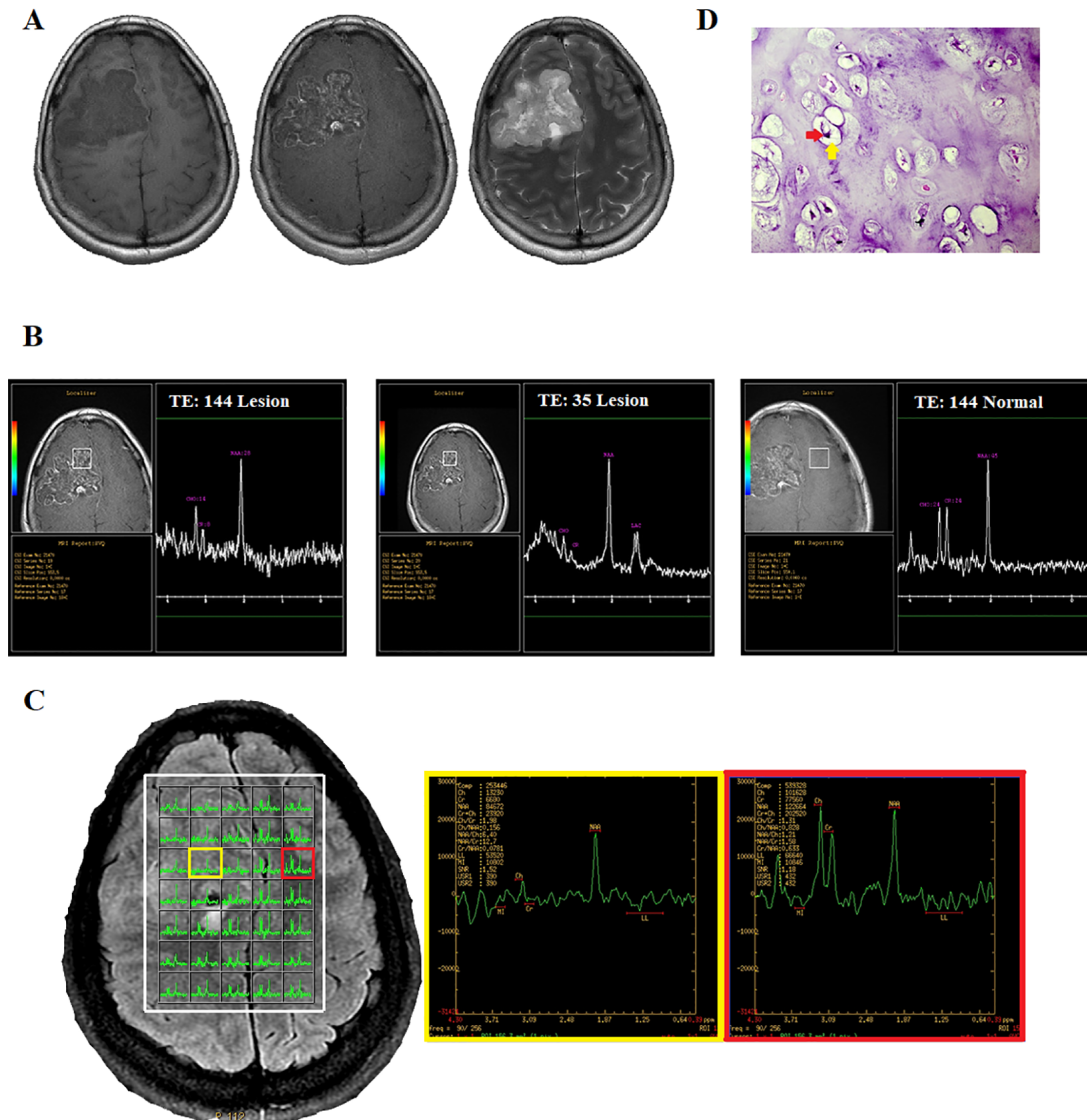


Figure 1. A 26-year-old woman with a chronic headache. A, Conventional MRI. B, Single-voxel spectroscopy (SVS). C, Multi-voxel MRS. D, Histopathologic examination shows the presence of mature cartilage tissue with a lobular architecture and bland-looking chondrocytes (red arrow), located in the lacuna (yellow arrow), confirming chondroma (H&E staining, 400 × magnification).

pathologic evaluation indicated the cartilaginous origin of the tumor, suggesting a chondroma (Figure 1D).

Histopathological findings and tumor pathology were reported by two pathologists in two different centers. After surgery, the patient's headache subsided, and no other signs or symptoms were reported. The whole-body assessment revealed no evidence of chondroma in other parts of the body. In the follow-up period, the patient reported no further complaints, and no neurological

deficits were detected.

2.2. Case 2

A 37-year-old male was admitted to our medical center due to a chronic progressive headache, left hemianesthesia, and left hemiparesis. The patient reported that his headache had begun approximately five months prior to his admission and that he had no history of trauma or exposure to radiation. The initial

physical examination revealed decreased muscle forces in the left extremities (4/5). Other neurological examinations were normal. Imaging was performed using a GE Optima 1.5 Tesla Scanner (GE Healthcare). The conventional brain MRI scans, including T1-weighted pre- and post-contrast, T2-weighted, T2-FLAIR, and diffusion-weighted imaging (DWI), showed a right-sided, parasagittal, ring-enhancing, solid-cystic, intra-axial lesion with significant edema in the posterior portion of the lesion (Figure 2A) and restriction in DWI images (data not shown).

Next, MRS was carried out in a single voxel (Figure 2B) and multivoxel using 3D chemical shift imaging (CSI) (Figure 2C). The SVS sequence parameters were the same as those in case 1. The voxel was located inside the lesion and the main H-MRS peaks, including Cho (3.2 ppm), Cr (3.03 ppm), myo-inositol (3.6 ppm), lipid (1.3 ppm), and a single peak at 2.02 ppm, were visible (Figure 2D). The quality of spectra was reported to be adequate for diagnostic evaluations. In the SVS-144 of the lesion side, a decrease in the peak at 2.02 ppm (with a value of 34 compared to the contralateral normal value of 44) and an increase in the Cho peak (with a value of 31 compared to the contralateral normal value of 21) were seen (Figure 2B). Also, the Cr level of the lesion was 19 as compared to the normal value of 21. The Cho/Cr ratio was 1.6 in the lesion. There were no distinct reverse peaks at 1.3 ppm in the moderate TE scan; therefore, the peak at 1.3 ppm in the SVS-35 scan was likely to be a lipid peak.

The 3D CSI sequence produced an $8 \times 8 \times 8$ transversely oriented matrix that was defined by a phase encoding scheme with FOV of 10×10 cm, resulting in an individual voxel size of $12.5 \times 12.5 \times 80$ mm. In the CSI data, the reduction of all metabolites was seen in the cystic portion of the lesion, while in some of these voxels, the lipid peak was a distinct single peak, which was correlated to necrosis transformation and/or tumor aggressiveness. In some parts of the solid lesion (in the same location as the single voxel), an elevation in the Cho peak was observed, and the Cho/Cr ratio was measured to be 2.35. However, there was no significant reduction in the peak of 2.02 at this voxel, and the Cho/NAA ratio was 0.8 (Figure 2C).

The elevation in the Cho peak, the presence of lipids, a Cho/Cr ratio of up to 2.35 in the CSI scan, and the conventional MRI features all suggest the presence of a high-grade glioma. Regarding the peak at 2.02, the radiologist assumed that this metabolite was related to NAA signal leakage from the brain tissue;

therefore, for the final diagnosis, this metabolite was ignored. The surgeon's observation during surgery was suggestive of a cartilaginous tumor. A pathological study revealed the presence of malignant cartilage tissue, accompanied by focal atypia and myxoid changes, indicating chondrosarcoma. The diagnosis was confirmed by an immunohistochemistry (IHC) study (Figure 2D). The histopathological findings and tumor pathology were reported by two independent pathologists in two different centers.

The follow-up evaluations showed that the patient no longer experienced headaches and had improved strength in their limbs. Moreover, the whole body evaluation was normal, without any other tumor sites. The patient did not experience any problems for seven months after the surgery. However, after this period, he was referred to our medical center due to seizures. The brain MRI with and without contrast showed evidence of an intra-axial mass-like lesion with a multi-cystic pattern in the right parietal lobe, without significant peripheral edema.

A brain MRS was conducted for presurgical planning. No diffusion restriction was observed in the DWI sequence, while in post-contrast images, abnormal enhancement of the lobular rim was detected in the surgical cavity. Additionally, slight enhancement was observed compared to primary MRI. Based on the spectra of different metabolites, such as NAA, Cr, and Cho, no significant increase was observed in the Cho/NAA ratio. Another surgical operation was performed to remove the tumor, and the pathological report of the extracted tissue indicated a recurrence of the tumor, consistent with a well-differentiated chondrosarcoma. After the surgery, the patient's symptoms improved, and he was transferred to the radiation oncology ward. During the six-month follow-up period, no signs or symptoms were reported.

3. Discussion

Here, we present two cases of intracranial cartilaginous tumors, including a chondroma and a chondrosarcoma. Intracranial chondromas and chondrosarcomas that do not originate from the skull base are extremely rare, and very few cases have been reported to date. Most previous cases mainly presented with a long-standing history of headaches and signs related to increased intracranial pressure. Based on

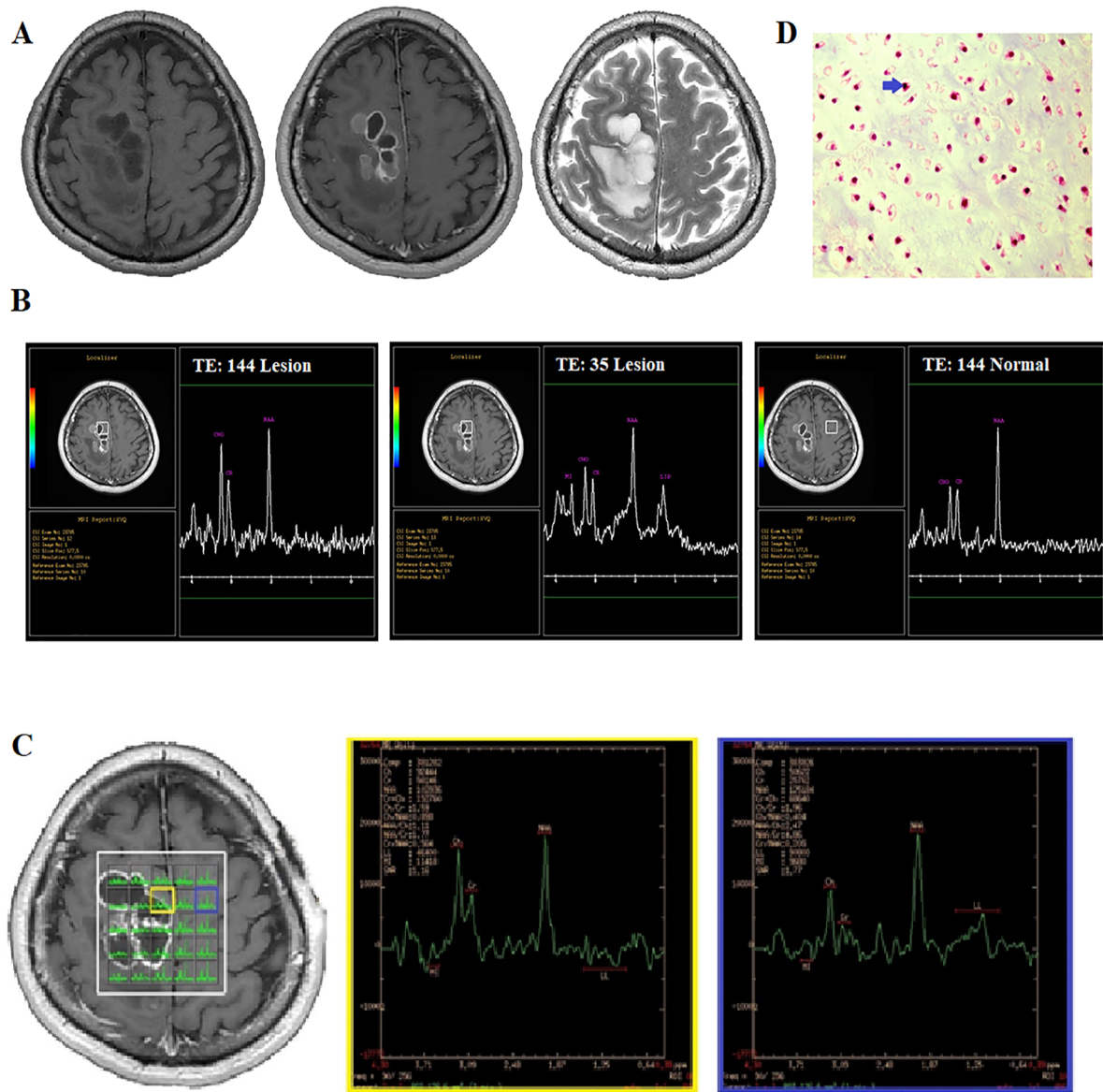


Figure 2. A 37-year-old man with a chronic progressive headache. A, Conventional MRI. B, Single-voxel spectroscopy (SVS). C, Multi-voxel MRS. D, Histopathological examination shows mature cartilage tissue with a lobular architecture, confirming neoplastic chondrocytic proliferation with mild atypia (blue arrow, H&E staining, 400 × magnification).

previous reports, these tumors were mainly diagnosed by brain CT scans and brain MRIs.

Previously reported MRI findings of intracranial chondrosarcomas include a densely enhancing mass with hypervascular features and a well-demarcated appearance that is hypointense on T1-weighted images and hyperintense on T2-weighted images. Additionally, these tumors often exhibit a heterogeneous pattern and are associated with edema (6). Chandler and colleagues

reported a 23-year-old female presenting with new-onset seizures due to an intracranial chondroma. It was recommended to conduct a careful analysis of brain imaging characteristics, as seen on CT scans or MRIs, for a correct diagnosis (7). In 2019, Agrawal and Saroha reported a case of intracranial chondroma and reviewed the clinical and imaging characteristics of previous cases. They showed that these tumors could appear homogeneous and isointense on T1-weighted images, with delayed or

slight ring-like enhancement on post-contrast images or as mixed hyper/hypointense masses on T2-weighted images (8).

In our first case, the primary brain MRI suggested an intracranial tumor, such as meningioma. However, it has been reported that contrast enhancement in meningioma is intensely homogeneous, while chondromas do not show homogeneous enhancement and may exhibit the dural tail sign (9). These findings demonstrate the significance of accurate radiologic reports in brain tumors for effective surgical planning. In this regard, Nikoobakht et al. presented a unique case of intracranial chondroma in a 19-year-old female patient, who was asymptomatic. The patient underwent a basic brain MRI and subsequently underwent surgery for tumor removal (10). Another study by Gunes et al. in 2009 reported a rare case of intracranial chondrosarcoma and described the imaging characteristics of the tumor (11). They reported that these tumors were isodense to hyperdense, with variable degrees of heterogeneous enhancement. Also, similar to our cases, these tumors were hypointense on T1-weighted MRI images and extremely hyperintense on T2-weighted MRI images (12).

In our study, imaging studies played an important role in the surgical planning of both cases. MRS is a non-invasive diagnostic test used to measure biochemical changes in the brain, particularly the presence of tumors. By comparing the frequency of each metabolite to normal brain tissue, radiologists can determine the type of tissue (13). An interesting imaging finding in our cases was the presence of an NAA-like peak on MRS images. Generally, NAA is a marker of normal neuronal function (14); therefore, its peak may be detected in non-neuronal tissues, such as extra-axial tumors. This occurs because of tissue heterogeneity in the voxel content. However, in our cases, especially case 1, a single voxel was localized inside the lesion; also, most of CSI voxels were occupied by the tumor tissue. Therefore, NAA contamination from brain tissue was excluded. The observed peak at 2 ppm corresponded to other N-acetylated metabolites produced by tumor cells, as previously reported in such rare lesions.

Moreover, Periakaruppan et al. reported some cases of colloid cysts with a sharp peak at 2 ppm. They found that these findings were correlated with the presence of NAA metabolites (15). Additionally, other reports of chondrosarcoma and chondroma and their MRS findings have been published (16-18). Table 1 presents a

brief report of these cases. Additionally, Kumaran et al. reported that in their case, the NAA-like peak at 2.02 ppm may be due to intralesional mucin, a hexosamine-rich glycoprotein, as evident on histopathology (16). Other spectroscopic findings of NAA-like peaks have been reported in metastatic brain tumors, originating from mucinous adenocarcinoma. The presence of a peak at 2.02 ppm could be related to other chemical compounds containing N-acetyl groups (19).

Our results, in concordance with previously reported cases, emphasized the diagnostic value of MRS. The common differential diagnosis for enhancing lesions in the brain, based on MRI features, is glial tumor. Therefore, the use of advanced imaging techniques could lead to more precise results. Generally, MRS has some limitations, such as having a low spatial resolution and being time-consuming. Nevertheless, the application of MRS for the detection of malignancies and tumors has increased in the past decades. Previous studies have reported the efficacy and beneficial outcomes of MRS in different tumors. Increased choline peak was observed in breast tumors, indicating the malignant and invasive behavior of the tumor in previous studies (20, 21).

In conclusion, our cases, as well as previous reports of chondroma and chondrosarcoma, suggest that conventional MRI findings may not provide accurate diagnoses for complex intracranial lesions. An important point to note in these cases is the similarity of symptoms, as well as the origin of both tumors from chondrocytes, which results in similar MRS patterns. The use of advanced neuroimaging techniques, such as MRS, may improve the diagnostic accuracy. However, MRS findings should be interpreted by expert radiologists due to the similarities of various metabolites. Also, report of rare cases worldwide can help improve radiographic diagnosis. In this report, the presence of a single peak at 2.02 ppm, despite the presence of a tumor lesion, was a distinct finding. However, further studies on a larger number of cases are needed to evaluate and diagnose lesions that produce other types of metabolites that are not yet known.

Footnotes

Authors' Contributions: B.A. drafted the manuscript; Sh.H. contributed to the design of the study and assisted in drafting the manuscript; A.P. referred the cases for imaging; M.I. reported the imaging results of one case; Y.B.

Table 1. A Few Reported Cases of Cartilaginous Intracranial Tumors Originating from Regions Other Than the Skull Base and Comparison with Our Cases

Authors	Age/sex	Clinical presentation	Tumor location	Conventional MRI findings	MRS findings	Histopathological findings
Fortuniak et al. (18)			Middle fossa	Hypointense on T1-weighted images and highly hyperintense on T2-weighted images	High lipid profile	Chondroma
Yeung et al. (17)	22/Female	Two episodes of seizure at four and 15 years of age	Parafalcine	An enhancing mass in the right frontal lobe with no significant vasogenic edema on T2-weighted and DWI images	Significant NAA, Cho, and Cr peaks, with a Cho/NAA ratio of 0.752	Chondroma
Kumaran et al. (16)	23/Female	Generalized tonic-clonic seizures and left-sided hemiparesis for one year	Right parietal convexity	Hypointense on T1-weighted images and heterogeneously hyperintense on T2-weighted images with no restricted diffusion on DWI	A single metabolite peak (a large peak at 2.02 ppm)	Grade I classic chondrosarcoma with interspersed areas of myxoid components
Our cases						
Case 1	26/Female	Chronic headache	Right frontal lobe (precentral and parasagittal)	An enhancing mass in T1 post-contrast images and hyperintense on T2-weighted images	SVS shows three peaks at 2, 3, and 3.2 ppm related to N-acetylated compounds, Cr, and Cho, respectively, with reduction in all metabolites compared to normal.	Chondroma
Case 2	37/Male	A chronic, progressive headache, left hemianesthesia, and left hemiparesis	Right frontal lobe (precentral and parasagittal)	Enhancing solid-cystic intra-axial lesions with significant edema	Elevation in Cho and lipid peaks, with the presence of an obvious peak at 2 ppm	Chondrosarcoma

Abbreviations: Cho, choline; Cr, creatinine; DWI, diffusion weighted imaging; NAA, N-acetylaspartate; SVS, single-voxel spectroscopy.

helped draft the manuscript; H.H. reported the imaging results of one case; M.O. revised the manuscript; E.N. reported the results of pathological assessments; and S.R. designed the study.

Conflict of Interests: The authors declare that they had no funding or research support, no employment, no personal financial interests, no stocks or shares in companies, no consultation fees, no patents, no personal or professional relations with organizations and individuals (parents and children, wife and husband, family relationships, etc.), no unpaid membership in a governmental or nongovernmental organization, Ahmad Pour-Rashidi and Elham Nazar are faculty members of Tehran University of Medical Sciences Samira Raminfarid is staff member of Tehran University of Medical Sciences Hassan Hashemi and Mohammad Ali Oghabian are editorial board members of the IJR, also they are faculty members of Tehran University of Medical Sciences.

Funding/Support: This work was funded by Tehran University of Medical Sciences (grant number: 51146).

Informed Consent: Written informed consent was

obtained from the cases reported in this study.

References

- Oktay K, Dere UA, Arslan M, Kesen S, Ciftci T. Intracranial chondroma without meningeal attachment. *Neurol India*. 2018;**66**(3):865-6. [PubMed ID: 29766963]. <https://doi.org/10.4103/0028-3886.232290>.
- Salek MAA, Faisal MH, Manik MAH, Choudhury A, Chowdhury RU, Islam MA, et al. Extra Skeletal Intracranial Chondroma of Falcine Origin: Case report and Review of Article. *Bang J Neurosurgery*. 2018;**7**(2):69-72.
- Ma X, Meng G, Wang K, Li D, Wang L, Li H, et al. The Differences Between Intracranial Mesenchymal Chondrosarcoma and Conventional Chondrosarcoma in Clinical Features and Outcomes. *World Neurosurg*. 2019;**122**:e1078-82. [PubMed ID: 30415056]. <https://doi.org/10.1016/j.wneu.2018.10.230>.
- Mahdavi A, Azar R, Shoar MH, Hooshmand S, Mahdavi A, Kharrazi HH. Functional MRI in clinical practice: Assessment of language and motor for pre-surgical planning. *Neuroradiol J*. 2015;**28**(5):468-73. [PubMed ID: 26443298]. [PubMed Central ID: PMC4757221]. <https://doi.org/10.1177/1971400915609343>.
- Shang HB, Zhao WG, Zhang WF. Preoperative assessment using multimodal functional magnetic resonance imaging techniques in patients with brain gliomas. *Turk Neurosurg*. 2012;**22**(5):558-65. [PubMed ID: 23015331]. <https://doi.org/10.5137/1019-5149.JTN.5332-11.1>.

6. Li L, Wang K, Ma X, Liu Z, Wang S, Du J, et al. Radiomic analysis of multiparametric magnetic resonance imaging for differentiating skull base chordoma and chondrosarcoma. *Eur J Radiol.* 2019;**118**:81-7. [PubMed ID: 31439263]. <https://doi.org/10.1016/j.ejrad.2019.07.006>.
7. Chandler JP, Yashar P, Laskin WB, Russell EJ. Intracranial chondrosarcoma: a case report and review of the literature. *J Neurooncol.* 2004;**68**(1):33-9. [PubMed ID: 15174519]. <https://doi.org/10.1023/b:neon.0000024728.72998.7d>.
8. Agrawal R, Saroha A. Intracranial Chondroma of the Falx Cerebri: A Rare Case Report with Review of Literature. *Asian J Neurosurg.* 2019;**14**(3):911-4. [PubMed ID: 31497127]. [PubMed Central ID: PMC6703020]. https://doi.org/10.4103/ajns.AJNS_82_19.
9. Fountas KN, Stamatiou S, Barbanis S, Kourtopoulos H. Intracranial falx chondroma: literature review and a case report. *Clin Neurol Neurosurg.* 2008;**110**(1):8-13. [PubMed ID: 17913345]. <https://doi.org/10.1016/j.clineuro.2007.08.020>.
10. Nikoobakht M, Shojaei H, Baseri YK, Shojaei SF. An Intraventricular Type of Chondroma: A Case Report. *Turk Neurosurg.* 2020;**30**(2):303-6. [PubMed ID: 30984997]. <https://doi.org/10.5137/1019-5149.JTN.25478-18.2>.
11. Gunes M, Gunaldi O, Tugcu B, Tanriverdi O, Guler AK, Colluoglu B. Intracranial chondrosarcoma: a case report and review of the literature. *Minim Invasive Neurosurg.* 2009;**52**(5-6):238-41. [PubMed ID: 20077365]. <https://doi.org/10.1055/s-0028-1128117>.
12. Kothary N, Law M, Cha S, Zagzag D. Conventional and perfusion MR imaging of parafalcine chondrosarcoma. *AJNR Am J Neuroradiol.* 2003;**24**(2):245-8. [PubMed ID: 12591641]. [PubMed Central ID: PMC7974122].
13. Zarifi M, Tzika AA. Proton MRS imaging in pediatric brain tumors. *Pediatr Radiol.* 2016;**46**(7):952-62. [PubMed ID: 27233788]. <https://doi.org/10.1007/s00247-016-3547-5>.
14. Munoz Maniega S, Cvorovic V, Chappell FM, Armitage PA, Marshall I, Bastin ME, et al. Changes in NAA and lactate following ischemic stroke: a serial MR spectroscopic imaging study. *Neurology.* 2008;**71**(24):1993-9. [PubMed ID: 19064881]. <https://doi.org/10.1212/01.wnl.0000336970.85817.4a>.
15. Periakaruppan A, Kesavadas C, Radhakrishnan VV, Thomas B, Rao RM. Unique MR spectroscopic finding in colloid-like cyst. *Neuroradiology.* 2008;**50**(2):137-44. [PubMed ID: 17987286]. <https://doi.org/10.1007/s00234-007-0324-z>.
16. Kumaran SP, Assis ZA, Viswamitra S, Ghosal N, Narayanam SK. N-acetyl aspartate peak in extra-axial extraosseous chondrosarcoma of the brain on MRI: Unravelling a diagnostic dilemma. *Neurol India.* 2016;**64**(1):176-8. [PubMed ID: 26755017]. <https://doi.org/10.4103/0028-3886.173640>.
17. Yeung JT, Krznarich TS, Moreno EA, Mulkamala A, Karim AS. Intracranial parafalcine chondroma in a pregnant patient. *Surg Neurol Int.* 2012;**3**:44. [PubMed ID: 22574253]. [PubMed Central ID: PMC3347491]. <https://doi.org/10.4103/2152-7806.94930>.
18. Fortuniak J, Jaskolski DJ, Stefanczyk L, Zawirski M, Gajewicz W. Magnetic resonance imaging of rare intracranial neoplasms-role of the in vivo 1 h spectroscopy in the radiological differential diagnostics. *Cent Eur Neurosurg.* 2010;**71**(4):181-8. [PubMed ID: 21082514]. <https://doi.org/10.1055/s-0030-1261947>.
19. Abdul Aziz Z, Jethwani D, Ananta Ram G, Sharath Kumar GG, Saini J. N-acetyl peak in proton MR spectroscopy of metastatic mucinous adenocarcinoma of brain. *Clin Neuroradiol.* 2013;**23**(2):153-6. [PubMed ID: 22367353]. <https://doi.org/10.1007/s00062-012-0137-2>.
20. Geraghty PR, van den Bosch MA, Spielman DM, Hunjan S, Birdwell RL, Fong KJ, et al. MRI and (1)H MRS of the breast: presence of a choline peak as malignancy marker is related to K21 value of the tumor in patients with invasive ductal carcinoma. *Breast J.* 2008;**14**(6):574-80. [PubMed ID: 19000051]. [PubMed Central ID: PMC2842578]. <https://doi.org/10.1111/j.1524-4741.2008.00650.x>.
21. Chen JH, Mehta RS, Baek HM, Nie K, Liu H, Lin MQ, et al. Clinical characteristics and biomarkers of breast cancer associated with choline concentration measured by 1H MRS. *NMR Biomed.* 2011;**24**(3):316-24. [PubMed ID: 20862660]. [PubMed Central ID: PMC3075960]. <https://doi.org/10.1002/nbm.1595>.